20

# Application of high-resolution terahertz spectroscopy to study the chemical composition of thermal decomposition products of bladder cancer tissues

© V.L. Vaks[1,2], V.A. Anfertev[1], E.G. Domracheva[1,2], M.B. Chernyaeva[1,2], V.A. Atduev[3,4], K.A. Atduev[3], A.S. Cherniaeva[1]

[1] IPM RAS,
Nizhny Novgorod, Russia
[2] Lobachevsky State University,
Nizhny Novgorod, Russia
[3] FBUZ POMC FMBA,
Nizhny Novgorod, Russia
[4] FSBEI HE „PRMU“,
Nizhny Novgorod, Russia
e-mail: elena@ipm.sci-nnov.ru

*Received October 31, 2025*
*Revised November 17, 2025*
*Accepted November 25, 2025*

Due to the need to detect oncological diseases at an earlier stage, when timely surgical or therapeutic treatment increases the likelihood of patient survival, it is urgent to search for and develop effective diagnostic and therapeutic strategies. Approaches based on metabolomics have the potential to identify sets of metabolite markers of cancer, which is important for early cancer recognition. One of the types of cancer that are difficult to detect in the early stages in modern conditions is urothelial cancer, for which the metabolic approach is promising in the early stages. The work is devoted to the study of the chemical composition of thermal decomposition products of primary metabolites for bladder tumor tissues, conducted for the first time using high-resolution THz spectroscopy methods.

**Keywords:** bladder cancer, biological tissue, thermal decomposition products, metabolites, high-resolution THz spectroscopy.

DOI: 10.61011/EOS.2025.12.63185.47-25

## Introduction

Bladder cancer (BC) is a significant component of urological cancer, characterized by a high potential for local recurrence and progression. The leading etiological factor in this disease is smoking, which is associated with exposure to aromatic amines and polycyclic hydrocarbons in tobacco smoke [1]. Work in the dyeing, rubber, oil, and other industries that involve contact with aromatic amines also plays a significant role [2]. Other established risk factors include consumption of water with high levels of arsenic or chlorination by-products [3], use of certain medications (cyclophosphamide [4], pioglitazone [5]), previous pelvic radiation therapy [6], schistosomiasis, and chronic cystitis [7].

As with all malignant tumors, the prognosis for patients with bladder cancer depends on the stage at the time of diagnosis. For example, the 5-year survival rate for non-muscle-invasive forms of BC (pTa, pT1, pTis) exceeds 90% [8], while it drops to 10% or lower for metastatic BC [9]. The current standard for the initial diagnosis of BC is cystoscopy followed by targeted biopsy or transurethral resection [10]. Despite their high accuracy, these methods are invasive, uncomfortable for the patient, and carry a risk of infectious complications. Urine cytology has extremely low sensitivity for detecting tumors with low malignant potential (G1–G2) [11]. Numerous non-invasive urinary tests (BTA, NMP22, UroVysion FISH, etc.), despite being approved for clinical use, do not have sufficient diagnostic accuracy, especially for detecting early stages of BC. Their widespread use is primarily limited because of insufficient specificity, which leads to false-positive results in the presence of inflammatory processes and other non-tumoral conditions [12]. BC can also be diagnosed using ultrasound and imaging techniques such as computed tomography (CT) or intravenous pyelogram, as well as radiographs (when contrast is used) to obtain detailed images [4,13]. However, all these methods have insufficient specificity.

In this regard, the development of new, highly accurate, and non-invasive diagnostic methods that can increase the BC detection rate at the earliest stages remains a significant challenge.

In this context, metabolomics is one of the most promising areas. The malignant transformation of a normal cell into a tumor cell is accompanied by a restructuring of its metabolism (Warburg effect, changes in the biosynthesis of nucleotides, lipids, and amino acids) [14], which is indicated by the qualitative and quantitative composition of metabolites (metabolome) both in the tumor tissue itself

and in the body's biological fluids [13]. Thus, the metabolic profile becomes a so-called „fingerprint" of a particular pathological process, which has a potentially high diagnostic value.

Research on the human metabolome and its biological components contributed to creation of an ever-growing Human Metabolome Database [15]. Since urine is one of the most easily accessible research objects that provides informative data about changes in the body's condition, the study of its metabolic composition is gaining significant attention worldwide. A database of specific urinary volatile substances has been created, containing 841 compounds from 80 chemical classes, some of which are associated with a number of cancerous diseases [16].

A number of reviews such as [17] described the metabolome of BC, including the metabolomes of both, fluids (urine and blood serum), cell lines, and tumor tissues; this review included a list of 1031 altered metabolites associated with the diagnosis and staging of BC, identified in human or mouse tissue samples based on a total of 25 selected studies. The research [18], where the high-resolution liquid chromatography was used in combination with mass spectrometry (LC–MS) and bioinformatic analysis to determine the global metabolome and lipidome of 25 BC tissue samples, showed that 533 metabolites were modified because of BC at low and high stages. In general, the modified metabolites included, among other things, nucleotides, polyamines, prostaglandins, and carnitines, while the modified lipids included seven distinct classes of lipids, namely cardiolipin, phosphatidylcholine, phosphatidylethanolamine, phosphatidylinositol, plasmenyl-phosphatidylethanolamine, phosphatidylserine, and triglycerides.

IPM RAS has developed gas spectroscopy methods using non-stationary effects in terahertz (THz) frequency range, distinguished by high resolution and sensitivity simultaneously, for the qualitative detection of products evolving from thermal decomposition of biological tissues and liquids [19,20]. Analysis of the spectroscopic measurements provides essential data on the differences in chemical composition of products evolved from thermal decomposition of healthy and pathological tissues, i.e., the products of the decomposition of large biological molecules during heating.

This study is aimed at conducting pilot studies of the chemical composition of primary metabolites thermal decomposition products for the bladder tumor tissues using high-resolution THz spectroscopy.

## Materials and methods

The spectra of the studied multicomponent gas mixtures were measured using a high-resolution THz non-stationary spectrometer developed by the authors [21]. As a result of the interaction of phase-switched (PS) radiation with resonantly absorbing gas molecules, a periodic process of induction and decay of molecules macroscopic polarization occurs. The resulting transient signals are registered and accumulated in the receiver part of the spectrometer. The magnitude and shape of these signals are used to determine the concentration of the gas mixture components with high accuracy. The spectrometer uses a phase-locked loop (PLL) system for automatic control of the backward-wave oscillator (BWO) frequency and phase shift. The transient process signal is registered in time, and then is averaged and processed by PC. The spectrometer can operate in two modes: fixed-frequency measurements and scanning mode. The analysis of recorded signals can be performed not only in the time domain, but also in the frequency domain after applying the Fourier transform to the original signal. Photo of the experimental setup is shown in Fig. 1 [21,22].

The package BWO OV-87 (118–178 GHz) was used as a radiation source. The power of BWO output signal reaches tens of milliwatts. After the inevitable losses in the waveguide nodes, the output signal power will still exceed 10 mW. BWO is powered by three high-stable DC power supplies — the cathode, grid, and filament, which

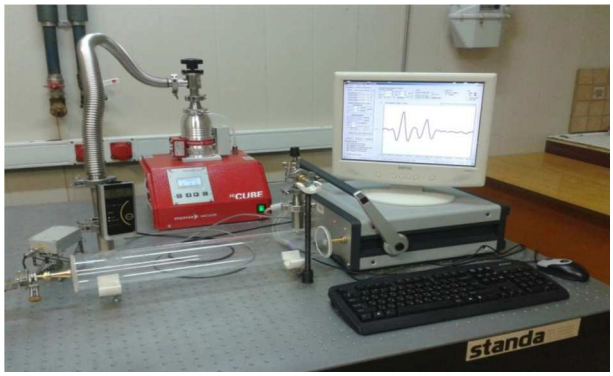


**Figure 1.** Photo of experimental setup on the basis of THz gas non-stationary spectrometer (118–178 GHz) [21,22].

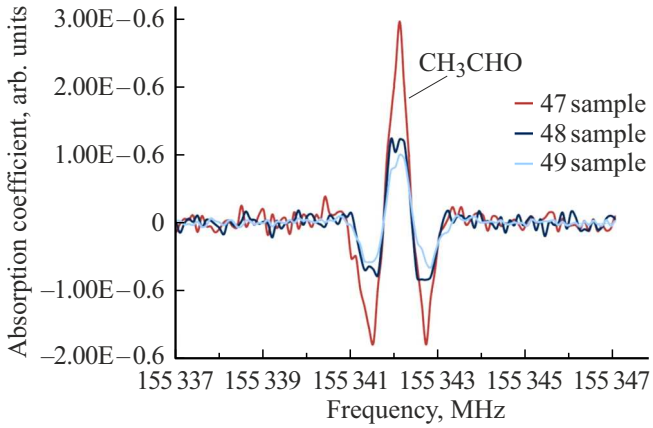


**Figure 2.** The acetaldehyde line ($CH_3CHO$), registered in mixtures of thermal decomposition products for three samples of bladder cancer tissue at a frequency of 155342.0881 MHz [23,24].

**Table 1.** Characteristics from the patients protocols

| Sample No. | Age- | Stage before operation | Stage after operation | IVCT/BCG /NAPCH | Relapse | Co-morbidities | Common urine analysis |
|---|---|---|---|---|---|---|---|
| 47 | 85 | cT1N0M0 | pT3bN0M0 | +/−/− | + | 1) HP II st., risk 3<br>2) Catarrhal colitis<br>3) Seropositive RA | PRO — 0.48 g/l,<br>WBC — 15 per power field;<br>RBC up to 100; VTC +++ |
| 48 | 78 | cT3bN0M0 | pT2bN1M0 | −/−/− | − | 1) HP II st., risk 3 | BAC +, WBC — 11 per power field |
| 49 | 65 | cT3bN0M0 | pT2bN1M0 | −/−/− | − | 1) Bubonocele in the left<br>2) Chronic hepatitis B infection | PRO — 1 g/l |

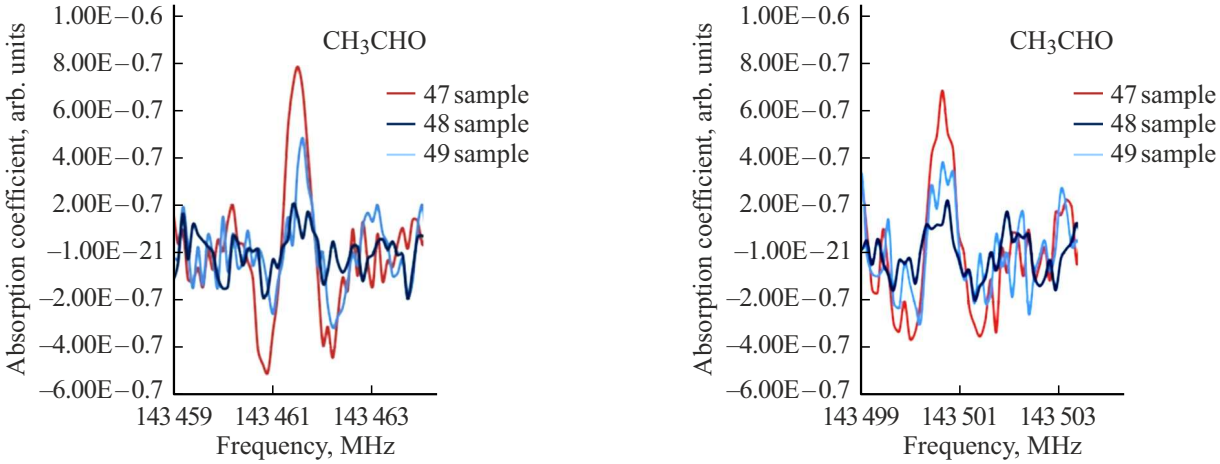


**Figure 3.** Lines of acetic acid ($CH_3COOH$), registered in mixtures of thermal decomposition products for three samples of bladder cancer tissue at a frequency 143461.5241 MHz [24] (in the left) and 143500.5243 MHz [24] (in the right).

have a low level of interference and noise (no more than a few millivolts), and have a short-circuit and high-voltage protection circuit. Output radiation frequency depends on the cathode power supply voltage and shall stay within 700−1600 V for a given frequency band. The grid and filament voltages are fixed at 200 and 1 V, respectively.

The device incorporates a 3-loop system of frequency synthesis. The first loop is a large-grid frequency-forming $F_r$ microwave frequency synthesizer. The second loop is a digital intermediate frequency synthesizer $F_{IF}$ that generates a fine frequency grid. And the third loop — BWO PLL system, incorporating BWO, directional coupler, harmonic mixer, intermediate frequency amplifier (IFA), and frequency-phase detector (FPD). In the third loop, the output frequencies generated by the first two loops are multiplied and mixed. BWO output frequency $F_{BWO} = NF_r - F_{IF}$, where $N$ — harmonic number of the reference frequency synthesizer signal, $F_r$ – frequency of the reference synthesizer, $F_{IF}$ — synthesizer frequency IF. The minimum frequency step at the output of the radiation source is determined by the minimum frequency step of the IF synthesizer. Both synthesizers have a common reference signal 10 MHz. To ensure frequency phase-switch (PS) at BWO output over the entire frequency range, the device uses phase-shift of the IF synthesizer signal and a wideband PLL, which allows for the transmission of PS without distortion from IF synthesizer to BWO output. The BWO frequency-locked loop system includes a directional coupler, a harmonic mixer, a low-noise local IFA, a frequency-phase detector, and a ferrite gate. The PLL control band in synchronization mode shall be at least 2.5 MHz over the entire BWO frequency band to transmit the PS of IF synthesizer to BWO output without distortion.

The receiving part of the device consists of an amplitude detector, a video amplifier, and a broadband ADC.

The study focused on tissue samples from malignant bladder tumors that were surgically removed and subjected to histological analysis. Data for the studied samples are given in Table 1 (where the following legends are used: IVCT — intravesicular chemotherapy, BCG —(Bacillus Calmette−Guerin) therapy, NAPCH — neoajuvant polychemotherapy, HP — hypertension, RA — rheumatoid arthritis, standard values of the common urine analysis: PRO – protein, WBC — leucocytes, RBC —erythrocytes, BAC – bacteria).

The method of studying the gas mixture components of the biological tissues thermal decomposition products, including sample preparation, was developed by the authors

**Table 2.** Chemical composition of vapors and products of thermal decomposition of samples of bladder cancer tumors

| Chemical compounds | Number of absorption lines in the sample spectrum, pcs. | | |
|---|---|---|---|
| | No. of sample | | |
| | 49 | 48 | 47 |
| Acetone with isotopologues | 4 | 3 | 2 |
| Hydroxyacetone | 7 | 2 | 5 |
| Dihydroxyacetone | 6 | 0 | 5 |
| Acetic acid | 61 | 26 | 25 |
| Isocyanic acidc with isotopologues | 19 | 10 | 9 |
| Methanol | 21 | 8 | 9 |
| Propanediol-1,2 | 11 | 7 | 6 |
| Propanediol-1,3 | 9 | 4 | 4 |
| Alaninol | 4 | 0 | 3 |
| Glycerol | 5 | 2 | 5 |
| Diethyl ether | 3 | 0 | 4 |
| Acetaldehyde with isotopologue | 89 | 55 | 64 |
| Propanal | 3 | 0 | 4 |
| Benzaldehyde | 2 | 4 | 7 |
| Glycolaldehyde with isotopologue | 2 | 4 | 4 |
| Malondialdehyde | 4 | 3 | 4 |
| Lactaldehyde | 4 | 2 | 2 |
| Acetonitrile | 11 | 6 | 10 |
| Ethyl cyanide with isotopologues | 25 | 5 | 21 |
| Propyl cyanide with isotopologues | 11 | 5 | 13 |
| Pentene nitrile | 11 | 4 | 12 |
| Benzonitrile | 4 | 1 | 5 |
| Methylbutyronitrile with isomer | 9 | 3 | 10 |
| 3,4-Pentadienenitrile with isomer | 7 | 6 | 5 |
| 2,4-Pentadienenitrile with isomer | 4 | 2 | 4 |
| Aminopropionitrile with isomer | 4 | 3 | 3 |
| Acrylonitril with isotopologue | 3 | 3 | 5 |
| Methylmercaptan with isotopologue | 43 | 51 | 58 |
| Alanine | 3 | 3 | 7 |
| Urea | 10 | 5 | 7 |
| Ethylene glycol | 5 | 3 | 3 |
| Glycinamide | 4 | 3 | 3 |
| Glycolamide | 4 | 3 | 3 |
| Acrylamide | 4 | 3 | 2 |
| Pyridine | 5 | 1 | 7 |
| Pyrrol | 16 | 2 | 16 |
| Cyanoethynylbenzene | 2 | 6 | 3 |
| Carbonyl sulfide with isotopologue | 14 | 13 | 17 |
| Sulfur dioxide with isotopologue | 23 | 10 | 12 |

earlier and described many times, e.g., in [19]. The essence of the approach is to heat the studied tissue sample to a temperature above 200°C and to put a mixture of thermal decomposition products into a measuring cell (quartz, 1 m long, pre-vacuumed) to a working pressure of about $5 \times 10^{-2}$mbar. After the scan, the spectrum was registered and saved in the spectrometer's computer. The spectrum is then analyzed to find the absorption lines, which are then identified using spectroscopic databases [23,24], and the number of absorption lines is counted for each chemical compound to provide a qualitative assessment of the compound's content in the mixture.

## Results

Table 2 provides summarized data on chemical composition of vapors and products of thermal decomposition of samples of bladder cancer tumors.

The spectra of all tumor tissue samples indicated such chemical compounds as organic acids (acetic acid, isocyanic acid with isotopologue), alcohols (methanol, two propanediol isomers), aldehydes (acetaldehyde, glycolaldehyde, malondialdehyde), nitriles (acetonitrile, pentadienenitrile with isomers, aminopropionitrile with isomer), sulfur-containing substances (methyl mercaptan, carbon dioxide with isotope, sulfur dioxide), a number of organic compounds (urea, ethylene glycol, glycinamide, glycolamide, acrylamide). The relative content of these substances was comparable for all three samples. Additionally, it should be noted that the spectra of two samples show a significant increase in the number of absorption lines compared to the third sample for substances such as propionitrile and butyronitrile with isotopologues, pentannitrile, methylbutyronitrile with an isomer, pyridine, and pyrrole.

Examples of characteristic absorption lines of acetaldehyde ($CH_3CHO$) and acetic acid ($CH_3COOH$) registered in mixtures of thermal decomposition products for three samples of bladder cancer tissue are shown in Figs. 2 and 3, respectively. Instrumental processing of data during non-stationary measurements of an absorption line results in the experimentally registered line having a shape similar to the second derivative of the Lorenz (or Voigt) line shape [25]. From Fig. 3, it can be seen that for sample 48, both absorption lines for the acetic acid are less intense, which indicates a slightly lower content of acetic acid in the studied thermal decomposition mixture for this sample.

## Conclusion

Thus, the potential of using high-resolution THz spectroscopy in the analysis of the metabolic composition of bladder neoplastic tissues was demonstrated. Substances that appear during the thermal decomposition of tumor tissue have been identified. A number of substances (acetic acid, acetaldehyde, etc.) have been identified that appear in significant relative amounts in the process of thermal

decomposition of the studied tumors and can be considered as potential markers of BC. In addition to identifying possible biomarkers at both the gene and molecular levels, there is a need to standardize protocols at all stages of experimental studies, combining appropriate experimental design with the cutting-edge analysis methods to improve reproducibility.

### Funding

This study was supported by the Russian Science Foundation (project No. 24-19-00623, https://rscf.ru/project/24-19-00623/).

### Conflict of interest

The authors declare no conflict of interest.

## References

[1] *IARC Working Group on the Evaluation of Carcinogenic Risks to Humans. Tobacco smoke and involuntary smoking.* IARC Monogr Eval Carcinog Risks Hum (International Agency for Research on Cancer, 2004), **83**, 1–143.
[2] S. Chavan, F. Bray, J. Lortet-Tieulent, M. Goodman, A. Jemal. Eur Urol., **66**, 59–73 (2014). DOI: 10.1016/j.eururo.2013.10.001
[3] M. Burger, J.W.F. Catto, G. Dalbagni, H.B. Grossman, H. Herr et al. Eur Urol., **63**, 234–241 (2013). DOI: 10.1016/j.eururo.2012.07.033
[4] C. Steinmaus, C. Ferreccio, J. Acevedo, Y. Yuan, J. Liaw et al. Cancer Epidemiol Biomarkers Prev., **23**, 1529–1538 (2014). DOI: 10.1158/1055-9965.EPI-14-0059
[5] M. Tuccori, K.B. Filion, H. Yin, O.H. Yu, R.W. Platt, L. Azoulay. BMJ, **352**, i1541 (2016). DOI: 10.1136/bmj.i1541
[6] K. Chrouser B. Leibovich, E. Bergstralh, H. Zincke, M. Blute, J. Urol., **174** (1), 107–110 (2005). DOI: 10.1097/01.ju.0000163459.57305.a1
[7] V.A. Moyer.Ann. Intern. Med., **155** (4), 246–51 (2011). DOI: 10.7326/0003-4819-155-4-201108160-00008
[8] M. Babjuk, M. Burger, O. Capoun, D. Cohen et al. Europ. Eur. Urol., **81** (1), 75–94 (2022). DOI: 10.1016/j.eururo.2021.08.010
[9] National Cancer Institute (NCI). SEER Cancer Stat Facts: Bladder Cancer, 2023. [Electronic source]. URL: https://seer.cancer.gov/statfacts/html/urinb.html
[10] *Campbell-Walsh-Wein Urology*, 12th Edition, ed. by A.J. Wein, T.F. Colon et al. (Elsevier, 2020).
[11] F.A. Yafi F Brimo, J. Steinberg, A.G. Aprikian, S. Tanguay, W. Kassouf. Urol. Oncol., **33** (66), e25 (2015). DOI: 10.1016/j.urolonc.2014.06.008
[12] V.B. Lokeshwar, T. Habuchi, H.B. Grossman, W.M. Murphy, S.H. Hautmann et al. Urology, **66**, 35–63 (2005). DOI: 10.1016/j.urology.2005.08.064
[13] M. Ahangar, F. Mahjoubi, S.J. Mowla. Front. Oncol., **14**, 1453278 (2024). DOI: 10.3389/fonc.2024.1453278
[14] M.G. Vander Heiden, L.C. Cantley, C.B. Thompson. Science, **324** (5930), 1029–1033 (2009). DOI: 10.1126/science.1160809
[15] Human Metabolome Database [Electronic source]. URL: www.hmdb.ca
[16] M. Llambrich, J. Brezmes, R. Cumeras. Biological Procedures Online, **24** (1), 20 (2022). DOI: 10.1186/s12575-022-00184-w
[17] F. Pereira, M.R. Domingues, R. Vitorino, I.M.S. Guerra, L.L. Santos, J.A. Ferreira, R. Ferreira. Int. J. Mol. Sci., **25**, 3347 (2024). DOI: 10.3390/ijms25063347
[18] V. Vantaku, J. Dong, C.R. Ambati, D. Perera, S.R. Donepudi, C.S. Amara, V. Putluri, S.S. Ravi, M.J. Robertson, D.W.B. Piyarathna et al. Clin. Cancer Res., **25**, 3689–3701 (2019). DOI: 10.1158/1078-0432.CCR-18-1515
[19] V. Vaks, E. Domracheva, M. Chernyaeva et al. J. Biophotonics, **18** (12), e202400316 (2024). DOI: 10.1002/jbio.202400316
[20] V. Vaks, E. Domracheva, M. Chernyaeva, V. Anfertev, A. Maslennikova, V. Atduev, K. Atduev, M. Rodionov.Appl. Sci., **14**, 1955 (2024). DOI: 10.3390/app14051955
[21] V.L. Vaks, V.A. Anfertyev, V.Yu. Balakirev, S.A. Basov, E.G. Domracheva, A.V. Illuk, P.V. Kupriyanov, S.I. Pripolzin, and M.B. Chernyaeva. Phys. Usp., **63** (7), 708–720 (2020). DOI: 10.3367/UFNe.2019.07.038613
[22] V.L. Vaks, E.G. Domracheva, M.B. Chernyaeva, V.A. Anfertyev, A.A. Ayzenshtadt, and A.V. Maslennikova, V.A. Atduev. *Teragerzevaya fotonika (300-year history of the Russian Academy of Sciences (RAS))* (RAS, M., 2023), p. 576–632 (in Russian).
[23] H.M. Pickett, E.A. Cohen, B.J. Drouin, J.C. Pearson et al. *Submillimeter, Millimeter, and Microwave Spectral Line Catalog. JPL Molecular Spectroscopy* (California Institute of Technology). http://spec.jpl.nasa.gov/ftp/pub/catalog/catform.html
[24] C.P. Endres, S. Schlemmer, P. Schilke, J. Stutzki, H.S.P. Müller. J. Mol. Spectrosc., **327**, 95–104 (2016). https://cdms.astro.uni-koeln.de/cgi-bin/cdmssearch
[25] W. Gordy, R.L. Cook. *Microwave molecular spectra* (J. Wiley&Sons, N.Y., 1984).

*Translated by J.Savelyeva*